Biosensors and Bioelectronics 145 (2019) 111673

Contents lists available at ScienceDirect

Biosensors and Bioelectronics

journal homepage: www.elsevier.com/locate/bios

A novel bionic *in vitro* bioelectronic tongue based on cardiomyocytes and microelectrode array for bitter and umami detection

Xinwei Wei[a,b], Chunlian Qin[a], Chenlei Gu[a], Chuanjiang He[a], Qunchen Yuan[a], Mengxue Liu[a], Liujing Zhuang[a], Hao Wan[a,b,**], Ping Wang[a,b,*]

[a] Biosensor National Special Laboratory, Key Laboratory for Biomedical Engineering of Education Ministry, Department of Biomedical Engineering, Zhejiang University, Hangzhou, 310027, China
[b] State Key Laboratory of Transducer Technology, Chinese Academy of Sciences, Shanghai, 200050, China

ARTICLE INFO

Keywords:
Bioelectronic tongue
Taste sensor
Cell-based biosensor
Cardiomyocyte
Microelectrode array

ABSTRACT

Electronic tongues (ETs) have been developed and widely used in food, beverage and pharmaceutical fields, but limited in sensitivity and specificity. In recent years, bioelectronic tongues (BioETs) integrating biological materials and various types of transducers are proposed to bridge the gap between ET system and biological taste. In this work, a bionic *in vitro* cell-based BioET is developed for bitter and umami detection, utilizing rat cardiomyocytes as a primary taste sensing element and microelectrode arrays (MEAs) as a secondary transducer for the first time. The primary cardiomyocytes of Sprague Dawley (SD) rats, which endogenously express bitter and umami taste receptors, were cultured on MEAs. Cells attached and grew well on the sensor surface, and syncytium was formed for potential conduction and mechanical beating, indicating the good biocompatibility of surface coating. The specificity of this BioET was verified by testing different tastants and bitter compounds. The results show that the BioET responds to bitter and umami compounds specifically among five basic tastants. For bitter recognition, only those can activate receptors in cardiomyocytes can be recognized by the BioET, and different bitter substances could be discriminated by principal component analysis (PCA). Moreover, the specific detections of two bitters (Denatonium Benzoate, Diphenidol) and an umami compound (Monosodium Glutamate) were realized with a detection limit of 10^{-6} M. The cardiomyocytes-based BioET proposed in this work provides a new approach for the construction of BioETs and has promising applications in taste detection and pharmaceutical study.

1. Introduction

Taste, or gustation, as one of the five basic sensations in mammals, plays an important role in identifying external environmental conditions. At present, it is widely believed that taste includes sour, salty, bitter, sweet and umami (Chandrashekar et al., 2006; Chaudhari and Roper, 2010). In recent years, fatty and metallic are also regarded as the basic taste sense in some research (Chale-Rush et al., 2007; Lawless et al., 2004). These basic tastes together constitute the taste space and play different roles in mammal life.

To mimic the biological taste sensing system, electronic tongues (ETs) have been intensively studied and developed in recent years, and have been widely used in food, beverage, pharmaceutical fields and water analysis (Baldwin et al., 2011; Escuder-Gilabert and Peris, 2010; Legin et al., 1999; Tahara and Toko, 2013). However, these artificial ETs based on electrochemical, optical or other sensors are limited in sensitivity and specificity compared with the biological taste system, which mainly lies on the biological receptor structures and information coding mechanisms (Ha et al., 2015). These years, the bioelectronic tongues (BioETs) integrating biological materials and various types of transducers are developed to bridge the gap between ET system and biological taste (Tønning et al., 2005), and have been applied in many fields such as food safety and water quality with high sensitivity and specificity (Cetó et al., 2016).

Due to the limitations of human taste system in the construction of BioET, researchers have utilized rat taste cells, taste epithelium and cell

* Corresponding author. Biosensor National Special Laboratory, Key Laboratory for Biomedical Engineering of Education Ministry, Department of Biomedical Engineering, Zhejiang University, Hangzhou, 310027, China.
** Corresponding author. Biosensor National Special Laboratory, Key Laboratory for Biomedical Engineering of Education Ministry, Department of Biomedical Engineering, Zhejiang University, Hangzhou, 310027, China.
E-mail address: cnpwang@zju.edu.cn (P. Wang).

https://doi.org/10.1016/j.bios.2019.111673
Received 28 April 2019; Received in revised form 22 August 2019; Accepted 2 September 2019
Available online 03 September 2019
0956-5663/ © 2019 Elsevier B.V. All rights reserved.

lines transfected with taste receptors to simulate the biological taste system. For example, Liu et al. employed microelectrode arrays (MEAs) to record electrophysiological activities of taste epithelium, establishing a novel taste sensor to investigate detection and recognition of basic tastes (Liu et al., 2013b). Chen et al. cultured taste receptor cells (TRCs) on the light addressable potentiometric sensor (LAPS) for specific sensation based on taste firing encoding (Chen et al., 2009). Similarly, Wu et al. discriminated different bitter compounds successfully by culturing TRCs on LAPS (Wu et al., 2012). Hu et al. expressed TAS2R16 taste receptor in heterologous HEK-293 cells, and electrical cell-substrate impedance sensing (ECIS) was used to detect the cellular status changes induced by salicin (Hu et al., 2017). Besides, artificial taste cell-derived nanovesicles, recombinant proteins and synthetic peptide also have been used for the construction of BioETs (Ahn et al., 2016; Lee et al., 2015; Son et al., 2017).

Recent studies have found that taste receptors are not only expressed in the gustatory system but also expressed in gastrointestinal and respiratory tracts of mammals, male reproductive system as well as in the brain and heart (Bezençon et al., 2006; Foster et al., 2013; Singh et al., 2011; Tizzano et al., 2011; Xu et al., 2012). Therefore, the wide expression of taste receptors provides a variety of possibilities for the construction of BioETs. For example, some researchers utilized the mouse germ cells (express Tas2rs) as sensitive elements, and combined cells with ECIS to construct a BioET for bitter detection (Hu et al., 2016). However, since the changes of cell morphology and impedance are an overall and slow process, these ECIS-based taste sensors respond slowly to the external tastants stimulation, which usually takes tens of minutes or longer. The long-time cost significantly limits the rapid recognition of taste compounds. Noteworthily, recent studies have demonstrated that cardiomyocytes in the heart of rats express taste receptors (bitter and umami receptors) (Foster et al., 2013). Therefore, cardiomyocytes that can produce electrical signals spontaneously might be used as biological materials for the tastant sensor, which has never been reported before as far as we know.

In this work, a bionic *in vitro* cell-based BioET is developed for bitter and umami detection, utilizing rat cardiomyocytes as a primary taste sensing element and microelectrode arrays (MEAs) as a secondary transducer for the first time. Fig. 1 shows the schematic diagram of the construction of BioET based on cardiomyocytes and MEAs. Cardiomyocytes of Sprague-Dawley (SD) rats were isolated and cultured on the surface of MEA sensor, which can record the electrophysiological signals of cardiomyocytes *in vitro*. Different kinds of taste compounds including bitter, sweet, sour, salty and umami were performed to verify the specificity of BioET, and principal component analysis (PCA) was applied to discriminate different tastants. Finally, the typical bitter and umami compounds were analyzed by this BioET.

2. Methods and experiments

2.1. Reagents and materials

Hanks Balanced Salt Solution (HBSS), Fetal Bovine Serum (FBS), Bovine Serum Albumin (BSA), Trypsin, and Collagenase Type II were purchased from Gibco (USA). Dulbecco's Modified Eagle Medium (DMEM), Calcein-AM, and Propidium iodide (PI) were purchased from Invitrogen (USA). Triton X-100 was purchased from Aladdin (USA). Phosphate-buffered saline (PBS), Paraformaldehyde (PFA), NaCl, Sucrose, Denatonium Benzoate (Dena), Diphenidol (Diph), Propylthiouracil (Prop), Phenyltiocarbamide (PTC) and Monosodium Glutamate (MSG) were purchased from Solarbio (China). Compounds solutions with different concentrations were prepared using culture medium. 1–2 days neonatal SD rats were purchased from Zhejiang Academy of Medical Sciences.

2.2. MEA sensor and detection system

MEA was proposed by Thomas to record the extracellular action potential of cells cultured *in vitro* in 1972 (Thomas Jr et al. 1972). After decades of development, MEA has become one of the most important biosensors currently. It can be used to monitor and evaluate the electrophysiological activities of electrogenic cells or tissues, which records the extracellular potential related to ionic transmembrane currents (Meyer et al., 2004; Pine, 2006).

MEA sensors were fabricated according to the concepts of micro-electro-mechanical systems (MEMS). The basic structure of sensor includes insulating substrate, metal electrode layer and passivation layer. All electrodes were fabricated by UV lithography, metal deposition, and lift-off processes. Platinum black was electroplated on the microelectrodes to increase surface area, reduce electrode impedance and improve the signal to noise ratio (SNR). Before experiment, the sensor chip was coated with 0.01% gelatin at 4 °C overnight to promote cell adhesion to MEAs. The detailed working principle diagram of MEAs is shown in Fig. S1. When cardiomyocytes produce action potentials spontaneously, transient transmembrane potentials and ionic currents are generated, and could polarize electrodes by reestablishing the charge distribution at electrode-electrolyte-cell interface and cause the change of electrode potential. In that way, the electric signal can be recorded by MEAs. The schematic diagram of MEA detection system is shown in Fig. 2a. Multi-electrode channels were wired out and connected to external modules that are used for signal amplification, filtering, data processing, and analysis. The potential signals of cardiomyocytes were recorded by electrodes, then processed by an amplifier and transmitted to the PC for display. The whole detection module with MEAs is put into the incubator with a stable environment to eliminate potential interference. Besides, there is also a temperature control module that helps control the temperature of the detection module. The actual measurement environment and set up of the recording system is shown in Fig. S2.

2.3. Cell culture

The experimental procedure of cell extraction and isolation refers to our previous work (Li et al., 2018; Wei et al., 2019). Ventricular tissue was isolated from neonatal SD rats. Then the tissue was transferred into a bottle with 2 mL HBSS and shredded into 1 mm^3 fragments. Tissue fragments were dissociated enzymatically by trypsin/collagenase type II mixture for 10–12 times. Cell suspension was centrifuged with 800 rpm for 5 min. The supernatant was removed and cells were re-suspended in 5 mL DMEM supplemented with 10% FBS. After 45 min differential attachment for 2 times, purified cardiomyocytes were obtained. The suspension was configured to appropriate cell density and cardiomyocytes were plated to the MEA at the density of 120,000 cells/cm^2. Cells were maintained in 37 °C and 5% CO_2 cell incubator. Cardiomyocytes would become mature in 3–5 days and can be used for electrophysiological signal recording. The medium was changed every 24 h. All protocols complied with regulations of Zhejiang University Institutional Animal Care and Use Committee (IACUC).

2.4. Live-dead cell staining

Calcein-AM (0.3 mg/L) and PI (0.5 mg/L), labelling live and dead cells respectively, were used to determine the cell viability of cardiomyocytes on MEA sensors. PBS was used to rinse samples after 20-min staining. Fluorescent images were taken by an inverted fluorescent microscope (NIB900, Nexcope, USA) at 37 °C in the dark environment.

2.5. Immunofluorescence staining

Cardiomyocytes were washed with 0.01M PBS and then fixed with 4% paraformaldehyde at room temperature (20–28 °C) for 30 min. With

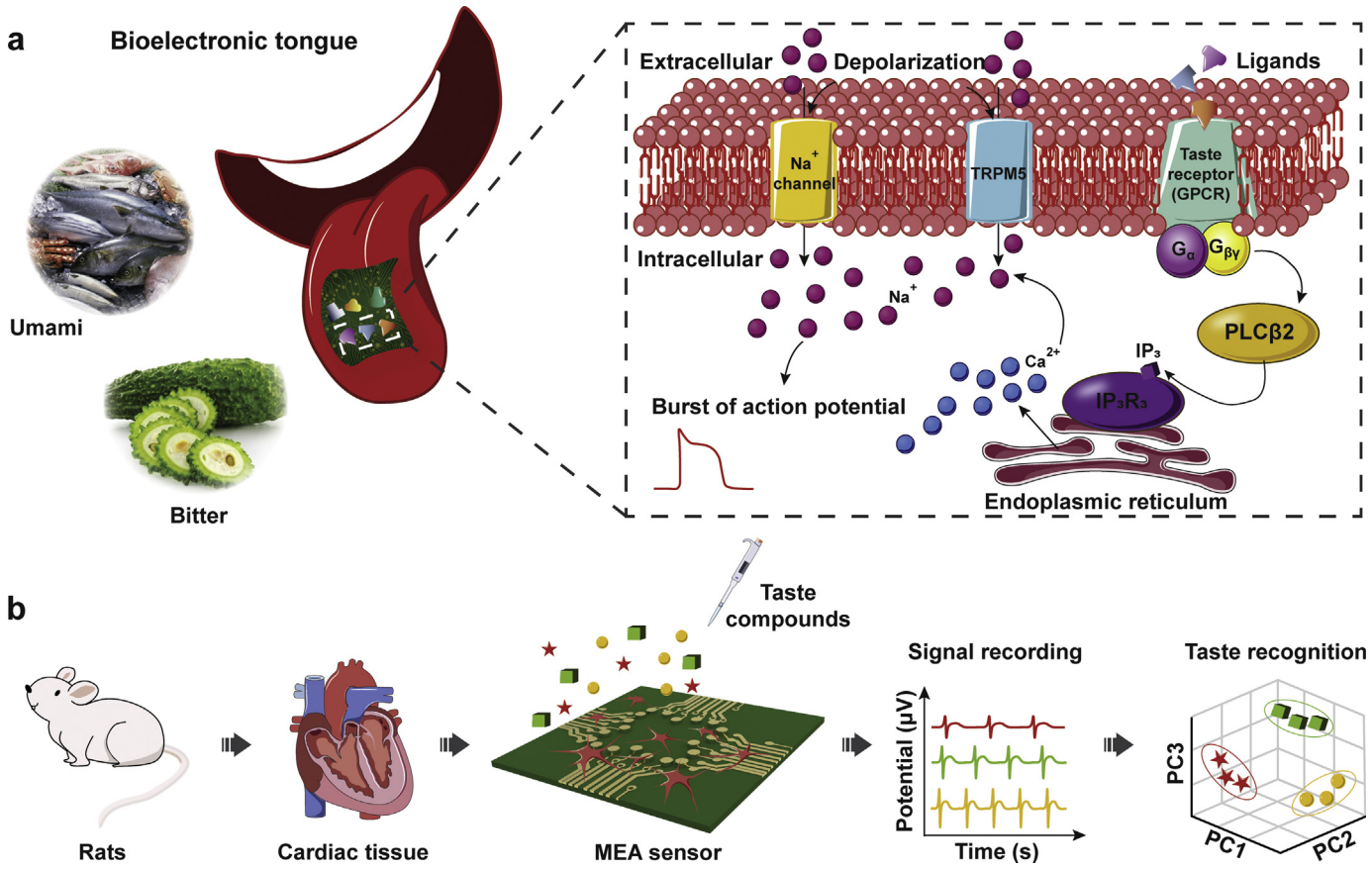

Fig. 1. (a) Schematic diagram of the BioET based on cardiomyocytes and MEA; (b) The construction of BioET and signal processing.

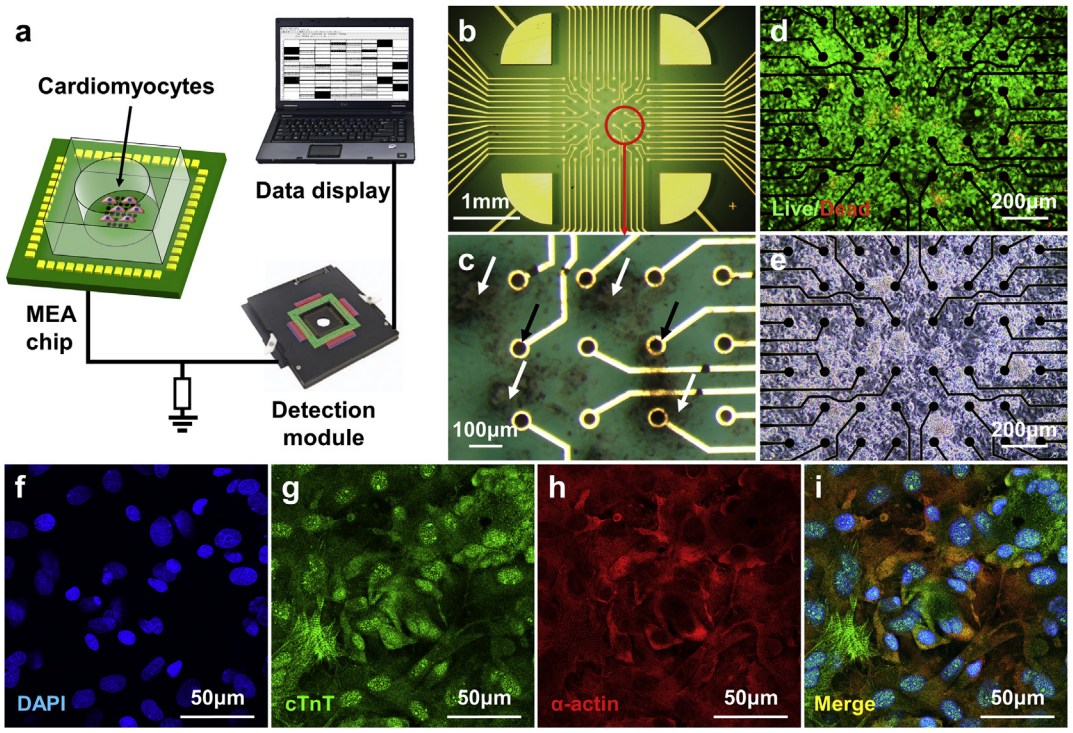

Fig. 2. (a) The schematic diagram of MEA detection system; (b) Electrodes configuration of MEA sensor; (c) Cardiomyocytes on MEA sensor; white arrows: cardiomyocytes; black arrow: electrode with platinum black; (d) Live/dead staining results of cardiomyocytes on MEA sensor; (e) Optical micrograph of cardiomyocytes on MEA sensor; (f–i) Immunofluorescence staining for DAPI (blue), cTnT (green) and α-actinin (red) in cardiomyocytes and the merged image. (For interpretation of the references to colour in this figure legend, the reader is referred to the Web version of this article.)

three times rinse by PBS buffer in between, the cells were permeabilized with 0.15% Triton X-100 (Aladdin) for 15 min and then incubated with a blocking solution of 1% BSA for 30 min at 37 °C. After that, cells were incubated with the primary antibody (Monoclonal Anti-α-Actin and Anti-Troponin T/cTnT) at 4 °C overnight. Subsequently, cells were washed with PBS three times before incubation with the secondary antibodies Cy3-labeled Goat Anti-Mouse IgG (H + L) at room temperature (20–28 °C) for 2 h. With the other three times rinse of PBS, the nuclei of the cells were stained by DAPI for 10 min. After nuclear staining with DAPI, α-actinin (a cardiomyocyte marker) and cardiac troponin T (cTnT), fluorescence images were captured by Laser confocal fluorescence microscopy (NIKON, Japan).

2.6. Data analysis

The MEA data was recorded and replayed in MC_Rack (Multi Channel Systems, Germany). The signals of all channels were analyzed by calculating signal amplitude, firing rate, duration time, interval time and so on. There may be a signal shape variation in different channels due to the cell separation process and different distribution of cells on the electrode (Yeung et al., 2007). To quantify and normalize the electrical signal across channels, data was normalized by the values of cardiomyocytes before the compound treatment (normalized value of control group is 1.00). The formula is shown below:

$$\text{Normalized value} = \frac{Value_{after\ treatment}(channel_i)}{Value_{control}(channel_i)}$$

All results and error bars were presented as mean ± standard deviation (SD). Data were performed by GraphPad Prism 6 (GraphPad Software Inc., USA) or Excel 2016 (Microsoft Corporation, USA). PCA was performed by MATLAB 2017 (MathWorks, Inc., USA).

3. Results and discussion

3.1. The principle of bioelectronic tongue based on cardiomyocytes and MEA

Among five taste sensations, the taste sensations of bitter, sweet and umami are mainly mediated by different types of G protein-coupled receptors (GPCRs) (Zhang et al., 2003). GPCRs are seven transmembrane-spanning proteins that mediate cellular and physiological responses by converting extracellular stimuli into intracellular signals. The taste receptor type 1 family (TAS1 in humans; Tas1 in rodents) mediate sweet (TAS1R2-TAS1R3) and umami (TAS1R1-TAS1R3) taste, while taste receptor type 2 (TAS2/Tas2) GPCRs mediate bitter taste. Besides in the gustatory system, taste receptors are also widely expressed in other tissues or physiological systems. Simon R. Foster et al. performed RT-qPCR taste receptor screens and found that two members of the Tas1 receptor family (Tas1r1 and Tas1r3) and seven Tas2 receptors (Tas2r108, Tas2r120, Tas2r121, Tas2r126, Tas2r135, Tas2r137, Tas2r143) were expressed in neonatal whole rat hearts (Foster et al., 2013). Moreover, taste receptors were more readily detected in primary rat cardiomyocytes than fibroblasts except for Tas1r3. These receptors lay the biological foundation for taste sensing based on cardiomyocytes. Therefore, rat cardiomyocytes were chosen as sensitive elements to build a BioET in this study.

Current studies have shown that the signalling pathways of three taste receptors (bitter, sweet and umami) are all mediated by GPCR (Zhang et al., 2003). As shown in Fig. 1a, when taste compounds bind to Tas1r or Tas2r receptor, the heterotrimeric G protein is activated, separating G_α (α-gustducin) and $G_{\beta\gamma}$. $G_{\beta\gamma}$ activates PLCβ2 to produce two intracellular messengers, IP_3 and diacylglycerol (DAG), which in turn release Ca^{2+} from the endoplasmic reticulum, causing an increase in intracellular Ca^{2+} concentration. Then Ca^{2+}-dependent TRPM5 channels are activated, which depolarizes the plasma membrane to generate action potentials and subsequent non-vesicular release of ATP (Taruno et al., 2013; Zhang et al., 2003). When taste ligands bind to the receptors on cardiomyocytes, action potentials generate due to the opening of ion channels, and the electronic signal can be recorded as extracellular field potential (EFP) by MEA sensor, which could be used to discriminate the different taste compounds.

3.2. Cardiomyocytes cultured on the MEA sensor

As shown in Fig. 2b, MEA sensor was designed as 8 × 8 array, consisting of 60 working electrodes (diameter is 30 μm and interelectrode distance is 200 μm) and 4 reference electrodes. After the separation and extraction, primary cardiomyocytes from SD rats were prepared into a cell suspension with appropriate density. Fig. 2c shows the attachment of cardiomyocytes on sensor chip cultured for 4 days. It can be found that cardiomyocytes (white arrows) attached on the sensor and distributed on or around the electrodes (black arrows), which is essential for electrodes to record the electrophysiological signals. Fig. 2d and e show the live/dead staining results and growth of cells under a microscope. We can see that most cells are live, which demonstrates the good biocompatibility of MEAs. Moreover, the beating of cardiomyocytes on MEA sensor chip could be observed under a microscope, indicating that syncytium was formed for potential conduction and mechanical beating. The cardiomyocytes used in this study were isolated from the whole heart of neonatal SD rats, so there may be some impurities cells like fibroblasts. Immunofluorescence staining results of cardiomyocytes are shown in Fig. 2f–i. The nuclei, cardiac troponin T (cTnT) and α-actinin (a cardiomyocyte marker) can be seen clearly in fluorescence images (blue, green and red, respectively). Thus immunofluorescence staining results verify the purity of isolated cardiomyocytes.

3.3. Specificity of bioelectronic tongue based on cardiomyocytes

3.3.1. The specific responses to bitter and umami compounds

It has been reported that bitter taste receptors (Tas2r) and umami taste receptors (Tas1r1 and Tas1r3) are expressed in cardiomyocytes. According to the principle of binding receptor to ligand, only bitter and umami compounds can activate the receptors on cardiomyocytes. To verify the specificity of BioET to bitter and umami substances, 5 kinds of taste compounds, including acid (0.1 mM HCl), salt (0.1 mM NaCl), sweet (0.1 mM Sucrose), bitter (0.1 mM Dena) and umami (0.1 mM MSG) were selected to test the performance of BioET. All these chosen compounds are prototypical tastants of corresponding taste qualities (Smith and St John, 1999).

After exposed to different tastants, the electrophysiological signals of cardiomyocytes were recorded in real-time. Fig. 3a shows the representative signals of cardiomyocytes after executed with different tastants. It can be found that the signals treated by Dena and MSG are significantly different from others. To analyze the signals more quantitatively, parameters including firing rate (FR), field potential amplitude (FPA), field potential duration (FPD), peak time, 50% rising time, 50% recovery time, 2nd peak time and interval time (the definition of parameters are shown in Fig. 3b) were extracted from data, and Fig. 3c shows the radar map of these parameters after normalization. As a result, FR and FPA present significant changes among the eight extracted parameters. Fig. 3d shows the statistics of normalized FR and FPA. It can be found that the normalized FR and FPA of sour, salty and sweet are similar to the control group, while the normalized values of bitter and umami are significantly different from others. In order to further investigate the signal differences, PCA was performed to discriminate the features of different taste response. Fig. 3e shows the 3D pattern clustering result based on the three principal components (cumulative contribution rate is 93.8%). It can be found that the signals are clustered into three regions, where signals under the stimulation of sour, sweet and salty compounds are located in the same region, while the

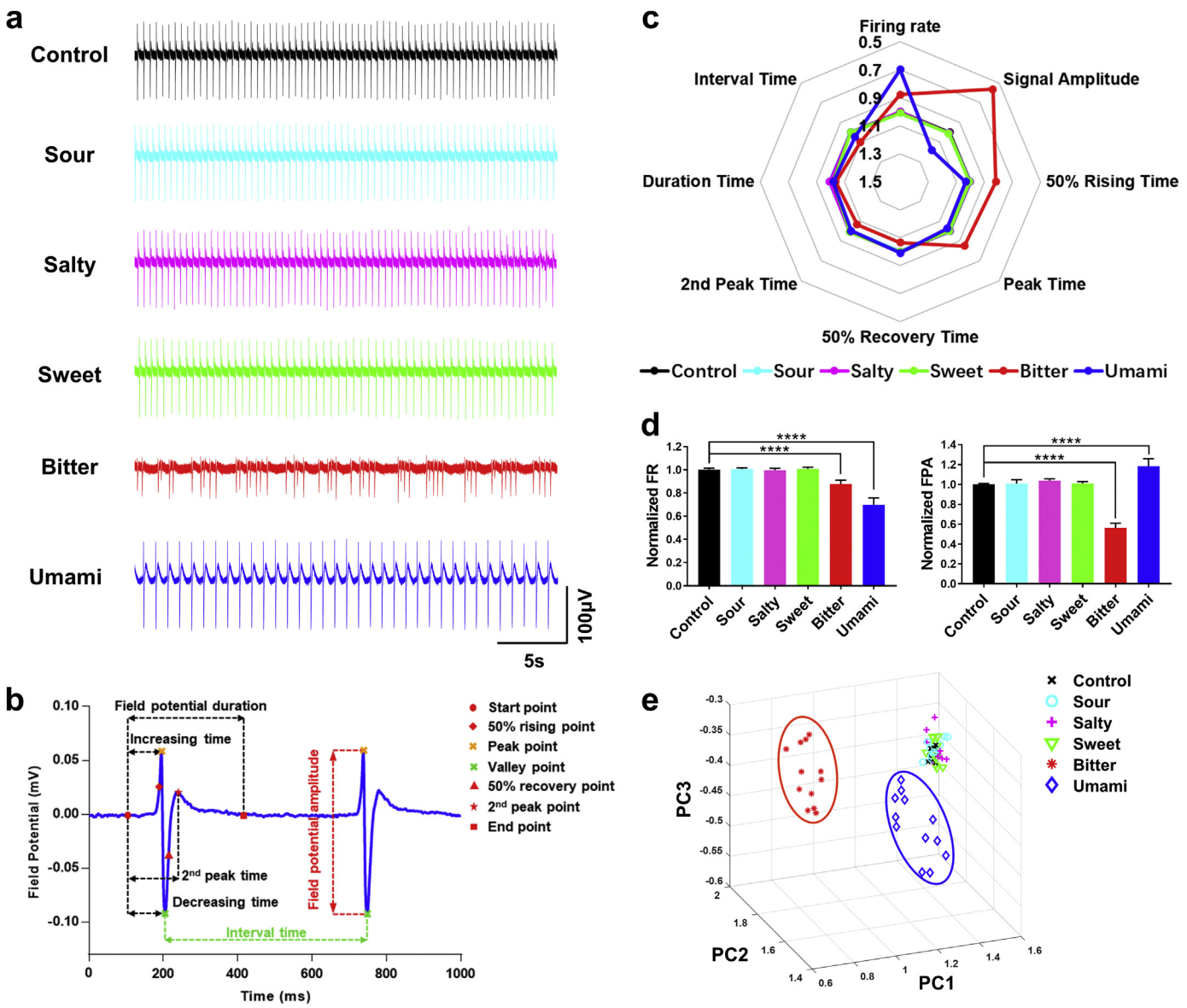

Fig. 3. (a) Typical signal of cardiomyocytes respond to different tastants, include 0.1 mM HCl (sour), NaCl (salty), Sucrose (sweet), Dena (bitter) and MSG (umami); (b) Typical spike signal and definition of parameters; (c) Radar map of extracted parameters; (d) Statistics of normalized FR/FPA after treated by different taste compounds (**, $P < 0.01$; ***, $P < 0.001$; ****, $P < 0.0001$; $n = 12$); (e) 3D pattern clustering result of different tastants based on PCA.

signals stimulated by bitter and umami substances are located in another two separate regions. The results above verify the specificity of cardiomyocytes-based BioET to bitter and umami compounds, and PCA is able to discriminate the bitter and umami substances.

3.3.2. *The specific responses to different kinds of bitter substances*

There are thousands of bitter substances in nature, different bitter compounds have various ligands that can bind to bitter receptors. Current researches have shown that a bitter substance can activate different kinds of receptors, and also a receptor can be activated by different ligands (Lossow et al., 2016). As the previous studies found, cardiomyocytes only express 7 kinds of Tas2r bitter receptors. So in theory, the bitter receptors on cardiomyocytes could only be activated by some certain bitter compounds. That is to say, cardiomyocytes-based BioET cannot respond to all substances but has certain specificity to some bitter compounds.

Bitter DB, established by the Hebrew University of Jerusalem, is a database about bitter-tasting natural and synthetic compounds and their cognate bitter taste receptors (Wiener et al., 2011). To verify the specificity of the taste sensor system, we searched for the ligands of receptors on cardiomyocytes through Bitter DB. Considering the expression quantity of receptors on cardiomyocytes and effective concentration of ligands, we selected Dena (activates Tas2r135), Diph (activates Tas2r108 and Tas2r137), and Prop (activates Tas2r108, Tas2r120, Tas2r121, Tas2r135 and Tas2r137) as three ligands, which can activate different receptors in cardiomyocytes. In contrast, PTC activates Tas2r138, which is not expressed in cardiomyocytes (Biarnés et al., 2010; Foster et al., 2013). Therefore, we expect that the BioET shows no response to PTC as well. To verify the specificity of BioET to bitterness, these four bitter compounds with the same concentration (100 μM) were exposed to cardiomyocytes, and electrophysiological signals of cells were recorded by MEAs. Similar to the method mentioned above, the parameters like FR and FPA of signals were extracted for PCA.

Fig. 4a shows the representative signals respond to different bitter compounds, and the radar map of extracted parameters is shown in Fig. 4b. It can be found that the changes of FR, FPA and interval time are most significant. Similarly, PCA was applied to differentiate the

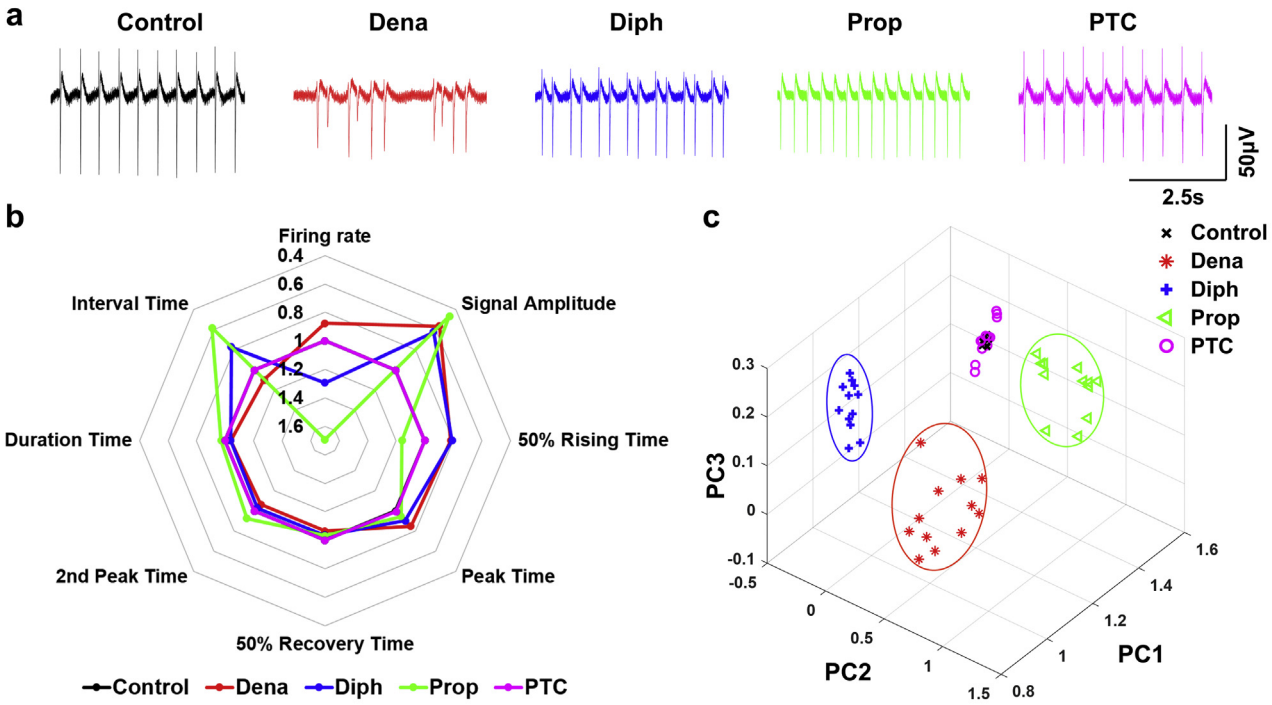

Fig. 4. (a) Typical signals respond to different bitter compounds; (b) Radar map of signal parameters of different bitter compounds; (c) 3D pattern clustering result of different bitter compounds based on PCA.

differences among different bitter substances more clearly. Fig. 4c shows the 3D pattern clustering result of three principal components (cumulative contribution rate is 95.7%). All signals are clustered into four regions, where the signals of control group and PTC are located in the same region, while the signals treated by Dena, Diph and Prop are located in another three different regions. The results indicate that The BioET has specific responses to Dena, Diph and Prop while has no significant response to the PTC. The signals respond to different bitter compounds could be discriminated by PCA in three-dimensional space.

The results above demonstrate the specificity of cardiomyocytes-based BioET to bitter substances that can activate the bitter receptors in cardiomyocytes, and different bitter substances can be discriminated by PCA.

3.4. Detection and analysis of bitter and umami compounds

3.4.1. Detection of Denatonium Benzoate

After verified the specificity, cardiomyocytes-based BioET was used for specific detection of different bitter and umami compounds. Dena can activate the Tas2r135 receptor in cardiomyocytes of rats (Lossow et al., 2016). Different concentrations (10, 20, 40, 80, 160, 320, 640 μM) of Dena were prepared to be administrated to the cardiomyocytes, respectively. The EFPs of cardiomyocytes were recorded in real-time. The typical EFP signals of cardiomyocytes after treated by different concentrations of Dena are shown in Fig. 5a. The results show that after the addition of Dena, the amplitudes of EFPs decrease with the increase of concentration, and electrical signals present a cluster-like emission trend. The Statistics of normalized FR and FPA are shown in Fig. 5c and d. It can be found that both the normalized FR and FPA decline. Moreover, normalized FR hardly shows linearity, while normalized FPA presents a linear change, with a linear fitting equation of $Y = -0.2878*X + 1.144$ and R^2 of 0.9846 (Fig. 5d). Thus normalized FPA was chosen to calculate the limit of detection (LOD). The working range covers at least from 10 μM to 640 μM. The LOD is calculated using the three-times standard deviation (SD) of the control group to inspect the ability of this *in vitro* BioET to distinguish valid signals from background noises. As a result, this BioET can detect Dena with a LOD of 3.46×10^{-6} M.

3.4.2. Detection of diphenidol

Diph can activate the Tas2r108 and Tas2r137 receptors in cardiomyocytes of rats (Lossow et al., 2016). Diph was prepared into different concentrations of 5, 10, 20, 40, 80, 160, 320 μM, and were added to the cardiomyocytes, respectively. The typical EFP signals of cardiomyocytes respond to different concentrations of Diph are shown in Fig. 5e. The statistical analysis of normalized FR and FPA are shown in Fig. 5g and h. It can be found that normalized FR shows no linearity while normalized FPA shows a linear decline with the increase of concentration. The linear fitting equation of normalized FPA is $Y = -0.3133*X + 1.136$, and R^2 is 0.9887 (Fig. 5h). Similarly, the LOD of Diph is calculated by three-times SD method. As a result, the LOD of Diph is 2.92×10^{-6} M.

Diphenidol has long been deployed as an anti-emetic and anti-vertigo drug, but its mechanism of action remains unclear. Some researchers have reported the electrophysiological effects of Diph on tissue or cells. For example, Hayakawa et al. found that Diph could result in depression of action potential amplitude, action potential duration and repolarization in Purkinje fiber (Hayakawa and Mandel, 1973). Leung et al. used patch-clamp method and found that Diph could block the voltage-gated Na^+ channels in neuronal cells, which contributed to diphenidol-induced spinal anesthesia in rats (Leung et al., 2010). In our research results, Diph has obvious inhibition effect on the potential amplitude of cardiomyocytes, which could relate to the blocking of Na^+ channels.

3.4.3. Detection of Monosodium Glutamate

MSG, a natural component in many foods, is an important gustatory stimulus and is believed to a signal dietary protein. MSG can activate the Tas1r1 and Tas1r3 taste receptors in cardiomyocytes (Chaudhari et al., 2000). Here, different concentrations of MSG (1, 10, 100, 1000, 4000, 5000, 6000 μM) were administrated to cardiomyocytes, respectively. Typical EFP signals of cardiomyocytes after the action of MSG

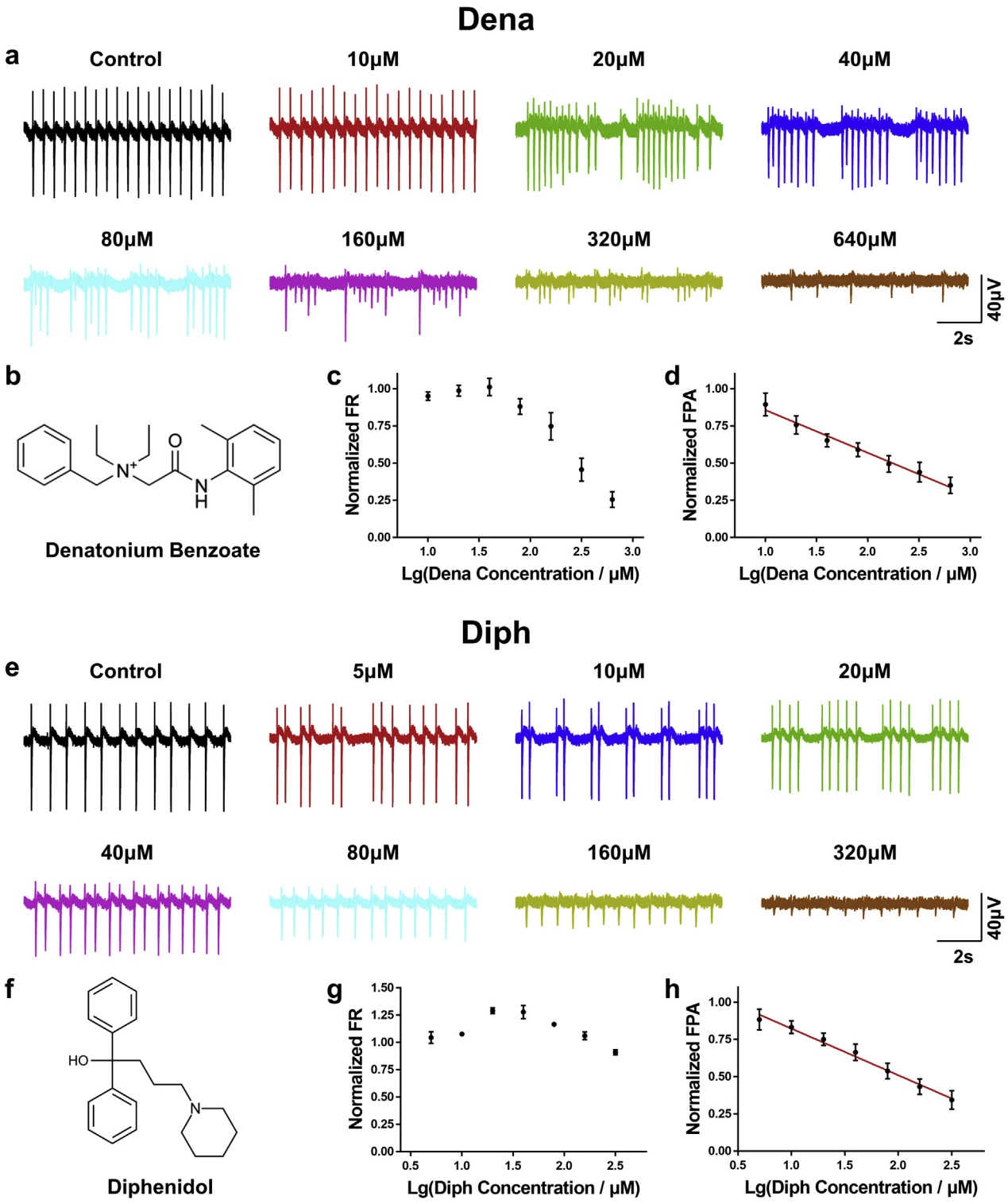

Fig. 5. (a) Typical EFP signals of cardiomyocytes respond to different concentrations of Dena (10–640 μM); (b) Chemical structure of Dena; (c–d) Statistics of normalized FR/FPA after Dena treatment with different concentrations; (e) Typical EFP signals of cardiomyocytes respond to different concentrations of Diph (5–320 μM); (f) Chemical structure of Diph; (g–h) Statistics of normalized FR/FPA after Diph treatment with different concentrations.

with different concentrations are shown in Fig. 6a and Fig. 6b.

The results show that at the concentration range of 1–4000 μM, the FR of EFPs drops first and then increase, while the FPA shows a concentration-dependent increase (Fig. 6a). It is worth noting that when the concentration of MSG is above 5000 μM, the firing rate of EFP increases rapidly within a very short time, followed by the inhibition and disappearance of signals (Fig. 6b). The speed of signal inhibition and disappearance at 6000 μM is faster than that at 5000 μM. But EFP signals of the cardiomyocytes could recover after eluting the MSG solution for an hour. Thus we guess the inhibition of EFP signals at high concentration may be related to the overload of cell ion channels.

Because of the inhibition at high concentration, the signals treated

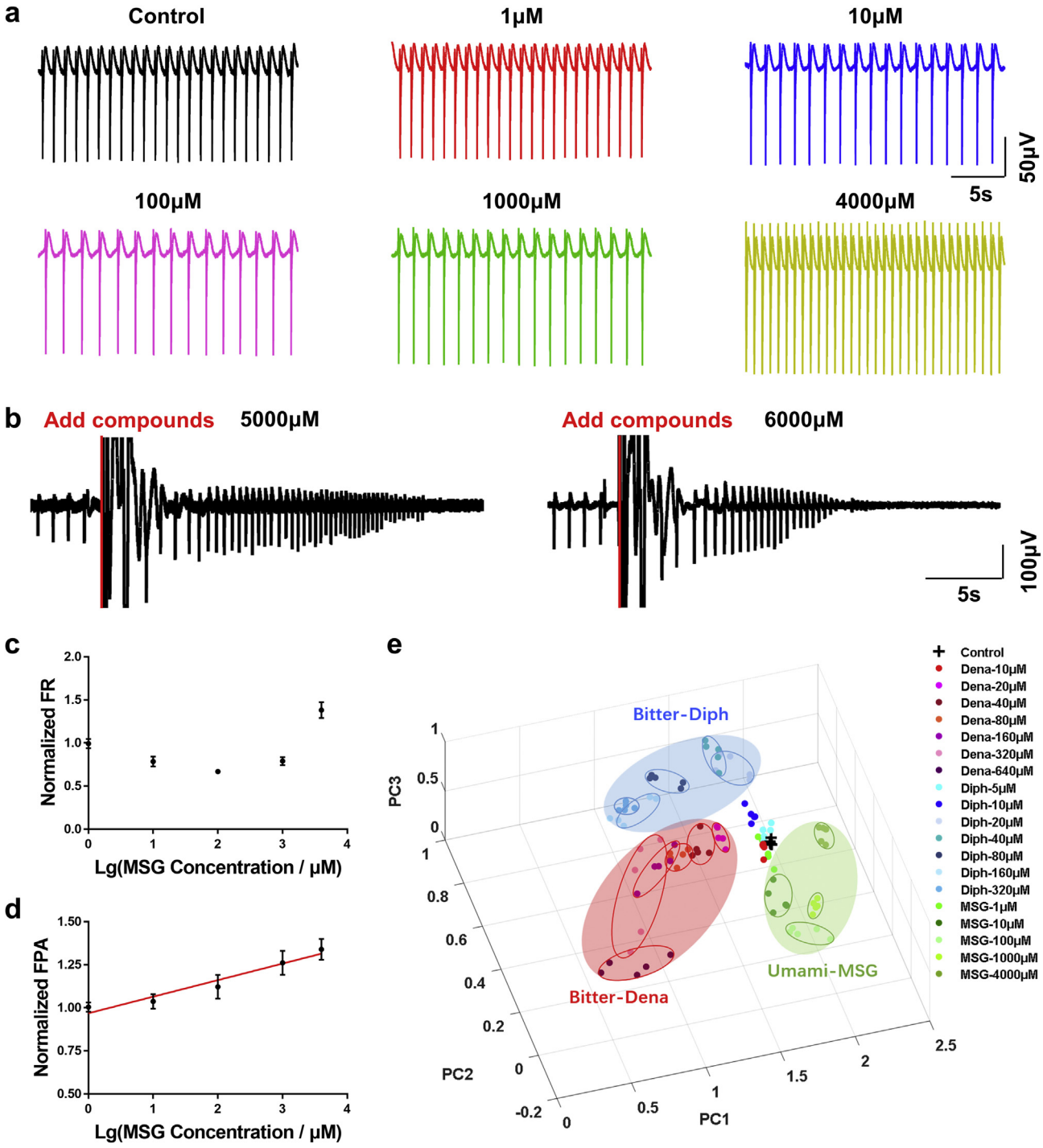

Fig. 6. (a) Typical EFP signals of cardiomyocytes respond to different concentrations of MSG (1, 10, 100, 1000, 4000 μM); (b) Typical EFP signals of cardiomyocytes respond to high concentrations of MSG (5000, 6000 μM); (c–d) Statistics of normalized FR/FPA after MSG treatment with different concentrations; (e) PCA result of different bitter and umami compounds with different concentrations.

by 1–4000 μM MSG were selected for statistical analysis. As shown in Fig. 6c, the normalized FR of EFP declines when the concentrations are below 1000 μM, then become bigger at the concentration of 4000 μM. Meanwhile, the normalized FPA of EFP presents a linear increase within the concentration range of 1–4000 μM (Fig. 6d). The linear fitting equation is $Y = 0.096*X + 0.968$, and R^2 is 0.9487. The LOD of MSG is 1.61×10^{-6} M through calculation.

Moreover, the data of Dena, Diph and MSG with different concentrations tested here were analyzed by PCA, and Fig. 6e shows the result based on the three principal components (cumulative contribution rate is 94.9%). It can be found that the data of the same compound with different concentrations are located in the same region, and the distance of bitter-bitter is smaller than that of bitter-umami, which indicates the correlation in bitter substances. Though the distance difference is relatively small at low or close concentrations, the data can be basically discriminated by PCA.

The LOD of BioET to bitter and umami compounds is 10^{-6} M in this work. Compared with commercially available ETs such as TS-5000Z/SA402B (Insent Inc., Atsugi-shi, Japan) and ASTREE2 (Alpha MOS, Toulouse, France), which can detect bitters (Caffeine, Quinine, Sodium

benzoate et al.) and umami (MSG) at 10^{-2}-10^{-5} M (Hayashi et al., 2008; Pein et al., 2013; Woertz et al., 2011; Yang et al., 2013), this BioET is more sensitive. Besides, our BioET also has advantages over the commercially available techniques in sensor fabrication cost and system complexity.

There are also other more sensitive BioETs based on recombinant proteins and graphene-based field-effect transistor (FET), which can detect MSG at 1 nM (Ahn et al., 2018). The LOD of our BioET is not as low as that work because of the different types of sensors and biomaterials. But compared with the work using cell-based biosensors, the results of our BioET is comparable or even superior to the previously reported results achieved by BioETs based on taste cells and taste epithelium, which can detect bitter tastants from 10 μM to 100 mM (Liu et al., 2013a) and umami tastants within 0.1–10 mM (Zhang et al., 2013). This cardiomyocytes-based BioET also remains its competitiveness compared with the BioET based on HEK-293 cells (transfected with taste receptors) and impedance sensor, which can detect bitter (Salicin) with a LOD of 0.055 mM. Moreover, taste sensor using cardiomyocytes (non-taste cells) has never been reported before as far as we know. This study is the first time to utilize cardiomyocytes and MEA sensor to construct a BioET, which can obtain more stable electric signals with high SNR compared with taste cells/epithelium-based BioET. This BioET also avoids the pretreatment of cell such as cell transfection compared with BioETs using other heterologous expression systems like bioengineered HEK-293 cells.

4. Conclusion

In this work, a bionic *in vitro* BioET based on cardiomyocytes and MEA was established for the detection of bitter and umami compounds for the first time. Bitter and umami taste receptors are endogenously expressed in cardiomyocytes, which lays the foundation of taste perception in cardiomyocytes. The primary cardiomyocytes of SD rats were cultured on MEAs, which were used to record the electrophysiological signals. Cells attached and grew well on the surface of sensor, and syncytium was formed for potential conduction and mechanical beating, indicating the good biocompatibility of surface coating. The BioET has specific responses to bitter and umami compounds among five basic tastants. For bitter recognition, only these ligands could activate the receptors in cardiomyocytes can be recognized, and different bitter substances could be discriminated by PCA. Moreover, the specific detections of two bitters (Dena, Diph) and an umami compound (MSG) were realized with a detection limit of 10^{-6} M. This study proposed a novel method to establish BioET based on cardiomyocytes and MEAs for the first time, which provides a new approach for the construction of BioETs and has promising applications in taste detection and pharmaceutical study.

CRediT authorship contribution statement

Xinwei Wei: Conceptualization, Investigation, Writing - original draft, Writing - review & editing, Visualization. **Chunlian Qin:** Writing - original draft, Methodology, Investigation. **Chenlei Gu:** Software, Formal analysis. **Chuanjiang He:** Methodology, Validation. **Qunchen Yuan:** Software, Visualization. **Mengxue Liu:** Formal analysis, Data curation. **Liujing Zhuang:** Writing - review & editing, Project administration. **Hao Wan:** Writing - original draft, Writing - review & editing, Supervision. **Ping Wang:** Conceptualization, Writing - review & editing, Supervision, Project administration, Funding acquisition.

Declaration of competing interest

The authors declare that they have no known competing financial interests or personal relationships that could have appeared to influence the work reported in this paper.

Acknowledgements

This work was supported by National Natural Science Foundation of China (No. 31571004, 31627801, 31661143030) and National 973 project (No. 2015CB352101). It is also grateful to Dr. Ning Hu for the kind help in paper writing.

Appendix A. Supplementary data

Supplementary data to this article can be found online at https://doi.org/10.1016/j.bios.2019.111673.

References

Ahn, S.R., An, J.H., Jang, I.H., Na, W., Yang, H., Cho, K.H., Lee, S.H., Song, H.S., Jang, J., Park, T.H., 2018. Biosens. Bioelectron. 117, 628–636.
Ahn, S.R., An, J.H., Song, H.S., Park, J.W., Lee, S.H., Kim, J.H., Jang, J., Park, T.H., 2016. ACS Nano 10 (8), 7287–7296.
Baldwin, E.A., Bai, J., Plotto, A., Dea, S., 2011. Sensors-Basel 11 (5), 4744–4766.
Bezençon, C., Le Coutre, J., Damak, S., 2006. Chem. Senses 32 (1), 41–49.
Biarnés, X., Marchiori, A., Giorgetti, A., Lanzara, C., Gasparini, P., Carloni, P., Born, S., Brockhoff, A., Behrens, M., Meyerhof, W., 2010. PLoS One 5 (8), e12394.
Cetó, X., Voelcker, N.H., Prieto-Simón, B., 2016. Biosens. Bioelectron. 79, 608–626.
Chale-Rush, A., Burgess, J.R., Mattes, R.D., 2007. Chem. Senses 32 (5), 423–431.
Chandrashekar, J., Hoon, M.A., Ryba, N.J., Zuker, C.S., 2006. Nature 444 (7117), 288.
Chaudhari, N., Landin, A.M., Roper, S.D., 2000. Nat. Neurosci. 3 (2), 113.
Chaudhari, N., Roper, S.D., 2010. J. Cell Biol. 190 (3), 285–296.
Chen, P., Wang, B., Cheng, G., Wang, P., 2009. Biosens. Bioelectron. 25 (1), 228–233.
Escuder-Gilabert, L., Peris, M., 2010. Anal. Chim. Acta 665 (1), 15–25.
Foster, S.R., Porrello, E.R., Purdue, B., Chan, H.-W., Voigt, A., Frenzel, S., Hannan, R.D., Moritz, K.M., Simmons, D.G., Molenaar, P., 2013. PLoS One 8 (5), e64579.
Ha, D., Sun, Q., Su, K., Wan, H., Li, H., Xu, N., Sun, F., Zhuang, L., Hu, N., Wang, P., 2015. Sens. Actuators B Chem. 207, 1136–1146.
Hayakawa, H., Mandel, W.J., 1973. J. Pharmacol. Exp. Ther. 185 (3), 447–456.
Hayashi, N., Chen, R., Ikezaki, H., Ujihara, T., 2008. J. Agric. Food Chem. 56 (16), 7384–7387.
Hu, L., Xu, J., Qin, Z., Hu, N., Zhou, M., Huang, L., Wang, P., 2016. Sens. Actuators B Chem. 223, 461–469.
Hu, L., Zou, L., Qin, Z., Fang, J., Huang, L., Wang, P., 2017. Sens. Actuators B Chem. 238, 1151–1158.
Lawless, H.T., Schlake, S., Smythe, J., Lim, J., Yang, H., Chapman, K., Bolton, B., 2004. Chem. Senses 29 (1), 25–33.
Lee, S.H., Lim, J.H., Park, J., Hong, S., Park, T.H., 2015. Biosens. Bioelectron. 71, 179–185.
Legin, A., Rudnitskaya, A., Vlasov, Y., Di Natale, C., Mazzone, E., D'Amico, A., 1999. Electroanalysis: An International Journal Devoted to Fundamental and Practical Aspects of Electroanalysis 11 (10-11), 814–820.
Leung, Y.-M., Wu, B.-T., Chen, Y.-C., Hung, C.-H., Chen, Y.-W., 2010. Neuropharmacology 58 (7), 1147–1152.
Li, H., Wei, X., Gu, C., Su, K., Wan, H., Hu, N., Wang, P., 2018. Anal. Sci. 34 (8), 893–900.
Liu, Q., Zhang, D., Zhang, F., Zhao, Y., Hsia, K.J., Wang, P., 2013a. Sens. Actuators B Chem. 176, 497–504.
Liu, Q., Zhang, F., Zhang, D., Hu, N., Hsia, K.J., Wang, P., 2013b. Biosens. Bioelectron. 43, 186–192.
Lossow, K., Hübner, S., Roudnitzky, N., Slack, J.P., Pollastro, F., Behrens, M., Meyerhof, W., 2016. J. Biol. Chem. 291 (29), 15358–15377.
Meyer, T., Boven, K.-H., Günther, E., Fejtl, M., 2004. Drug Saf. 27 (11), 763–772.
Pein, M., Eckert, C., Preis, M., Breitkreutz, J., 2013. J. Pharm. Biomed. Anal. 83, 157–163.
Pine, J., 2006. Advances in Network Electrophysiology. Springer, pp. 3–23.
Singh, N., Vrontakis, M., Parkinson, F., Chelikani, P., 2011. Biochem. Biophys. Res. Commun. 406 (1), 146–151.
Smith, D.V., St John, S.J., 1999. Curr. Opin. Neurobiol. 9 (4), 427–435.
Son, M., Kim, D., Ko, H.J., Hong, S., Park, T.H., 2017. Biosens. Bioelectron. 87, 901–907.
Tønning, E., Sapelnikova, S., Christensen, J., Carlsson, C., Winther-Nielsen, M., Dock, E., Solna, R., Skladal, P., Nørgaard, L., Ruzgas, T., 2005. Biosens. Bioelectron. 21 (4), 608–617.
Tahara, Y., Toko, K., 2013. IEEE Sens. J. 13 (8), 3001–3011.
Taruno, A., Vingtdeux, V., Ohmoto, M., Ma, Z., Dvoryanchikov, G., Li, A., Adrien, L., Zhao, H., Leung, S., Abernethy, M., 2013. Nature 495 (7440), 223.
Thomas Jr., C., Springer, P., Loeb, G., Berwald-Netter, Y., Okun, L., 1972. Exp. Cell Res. 74 (1), 61–66.
Tizzano, M., Cristofoletti, M., Sbarbati, A., Finger, T.E., 2011. BMC Pulm. Med. 11 (1), 3.
Wei, X., Gu, C., Li, H., Pan, Y., Zhang, B., Zhuang, L., Wan, H., Hu, N., Wang, P., 2019. Sens. Actuators B Chem. 283, 881–889.
Wiener, A., Shudler, M., Levit, A., Niv, M.Y., 2011. Nucleic Acids Res. 40 (D1), D413–D419.
Woertz, K., Tissen, C., Kleinebudde, P., Breitkreutz, J., 2011. Int. J. Pharm. 417 (1–2), 256–271.
Wu, C., Du, L., Mao, L., Wang, P., 2012. Journal of Innovative Optical Health Sciences 5 (02), 1250008.
Xu, J., Cao, J., Iguchi, N., Riethmacher, D., Huang, L., 2012. MHR: Basic science of

reproductive medicine 19 (1), 17–28.
Yang, Y., Chen, Q., Shen, C., Zhang, S., Gan, Z., Hu, R., Zhao, J., Ni, Y., 2013. J. Food Eng. 116 (3), 627–632.
Yeung, C., Sommerhage, F., Wrobel, G., Offenhäusser, A., Chan, M., Ingebrandt, S., 2007. Anal. Bioanal. Chem. 387 (8), 2673–2680.
Zhang, D., Zhang, F., Zhang, Q., Lu, Y., Liu, Q., Wang, P., 2013. Biochem. Biophys. Res. Commun. 438 (2), 334–339.
Zhang, Y., Hoon, M.A., Chandrashekar, J., Mueller, K.L., Cook, B., Wu, D., Zuker, C.S., Ryba, N.J., 2003. Cell 112 (3), 293–301.